XeCu Covalent Bonding in XeCuF and XeCuCl, Characterized by Fourier Transform Microwave Spectroscopy Supported by Quantum Chemical Calculations

Julie M. Michaud[†] and Michael C. L. Gerry*

Contribution from the Department of Chemistry, The University of British Columbia, 2036 Main Mall, Vancouver, British Columbia, Canada V6T 1Z1

Received January 31, 2006; E-mail: mgerry@chem.ubc.ca

Abstract: XeCu covalent bonding has been found in the complexes XeCuF and XeCuCl. The molecules were characterized by Fourier transform microwave spectroscopy, supported by MP2 ab initio calculations. The complexes were prepared by laser ablation of Cu in the presence of Xe and SF_6 or Cl_2 and stabilized in supersonic jets of Ar. The rotational constants and centrifugal distortion constants show the XeCu bonds to be short and rigid. The ^{131}Xe, Cu, and Cl nuclear quadrupole coupling constants indicate major redistributions of the electron densities of Xe and CuF or CuCl on complex formation which cannot be accounted for by simple electrostatic effects. The MP2 calculations corroborate the XeCu bond lengths and predict XeCu dissociation energies $\sim$50−60 kJ mol^{-1}. The latter cannot be accounted for in terms of induction energies. The MP2 calculations also predict valence molecular orbitals with significant shared electron density between Xe and Cu and negative local energy densities at the XeCu bond critical points. All evidence is consistent with XeCu covalent bonding.

1. Introduction

Since 1999, the preparation and characterization of a series of noble gas−noble metal halide complexes NgMX have been reported, where Ng = Ar, Kr, Xe; M = Cu, Ag, Au; and X = F, Cl, Br.[1−10] They were prepared by ablation of a metal rod with a Nd:YAG laser in the presence of suitable precursors, and the reaction products were stabilized in supersonic jets of Ar. A cavity pulsed jet Fourier transform microwave spectrometer was used to detect and characterize these complexes via their rotational spectra.

The noble gas−noble metal halides have all been found to be linear and have some interesting properties, consistent with unusually strong noble gas−noble metal interactions. The NgM bonds are short and rigid. Nuclear quadrupole coupling constants of ^{83}Kr, ^{131}Xe, Cu, Au, Cl, and Br indicate significant rearrangements of electron distribution on complex formation. Ab initio NgM dissociation energies are large[11] and have a monotonic relationship with experimental NgM stretching force constants. Ab initio calculations also show shared electron density between Ng and M atoms in occupied valence molecular orbitals (MOs) and significant donation of electron density from Ng to M. Recent calculations have provided local energy densities from which NgM covalent bonding character has been determined. These properties give an indication of the strengths of the interactions between Ng and M; they increase as Ng is changed from Ar to Kr to Xe and as M is changed from Ag to Cu to Au. The interactions of complexes containing XeCu and XeAu bonds would be most interesting because of their anticipated strengths. XeAuF has been reported earlier,[10] and this paper focuses on XeCuF and XeCuCl. These microwave spectroscopic measurements provide the first detection and characterization of complexes containing XeCu bonds.

2. Experimental Methods

The experiments were performed using a Balle−Flygare-type[12] Fourier transform microwave (FTMW) spectrometer with a laser ablation system at the mouth of the nozzle. Details of the FTMW spectrometer used have been given earlier, as have details of the laser ablation setup.[13] In the present work, a copper rod was ablated with pulses of radiation from a Nd:YAG laser (1064 nm) to produce a metal plasma. The rod was rotated and translated to ensure a fresh ablation surface for each laser pulse. Reactions occurred between the plasma and the precursors ($\sim$2% SF_6 or 0.1% Cl_2 with 10−20% Xe) entrained in Ar. The backing gas containing the precursors generally had a pressure of 5−7 atm. The reaction products were injected into the Fabry−Pérot cavity and were stabilized in the collision-free environ-

† Present address: Department of Chemistry, The University of Alberta, Edmonton, AB, Canada T6G 2G2.

(1) Evans, C. J.; Gerry, M. C. L. *J. Chem. Phys.* **2000**, *112*, 1321.
(2) Evans, C. J.; Gerry, M. C. L. *J. Chem. Phys.* **2000**, *112*, 9363.
(3) Evans, C. J.; Rubinoff, D. S.; Gerry, M. C. L. *Phys. Chem. Chem. Phys.* **2000**, *2*, 3943.
(4) Evans, C. J.; Lesarri, A.; Gerry, M. C. L. *J. Am. Chem. Soc.* **2000**, *122*, 6100.
(5) Walker, N. R.; Reynard, L. M.; Gerry, M. C. L. *J. Mol. Struct.* **2002**, *612*, 109.
(6) Reynard, L. M.; Evans, C. J.; Gerry, M. C. L. *J. Mol. Spectrosc.* **2001**, *206*, 33.
(7) Thomas, J. M.; Walker, N. R.; Cooke, S. A.; Gerry, M. C. L. *J. Am. Chem. Soc.* **2004**, *126*, 1235.
(8) Michaud, J. M.; Cooke, S. A.; Gerry, M. C. L. *Inorg. Chem.* **2004**, *43*, 3871.
(9) Cooke, S. A.; Gerry, M. C. L. *Phys. Chem. Chem. Phys.* **2004**, *6*, 3248.
(10) Cooke, S. A.; Gerry, M. C. L. *J. Am. Chem. Soc.* **2004**, *126*, 17000.
(11) Lovallo, C. C.; Klobukowski, M. *Chem. Phys. Lett.* **2002**, *368*, 589.

(12) Balle, T. J.; Flygare, W. H. *Rev. Sci. Instrum.* **1981**, *52*, 33.
(13) (a) Walker, K. A.; Gerry, M. C. L. *J. Mol. Spectrosc.* **1997**, *182*, 178. (b) Xu, Y.; Jäger, W.; Gerry, M. C. L. *J. Mol. Spectrosc.* **1992**, *151*, 206.

ment. Microwave radiation pulsed into the cavity rotationally polarized the samples. At the end of each pulse, a decay of the polarization was detected. A Fourier transform was used to convert the signal-averaged time domain signal into a frequency domain signal. The propagation of microwaves in the cavity was coaxial to the gas expansion, resulting in high sensitivity and resolution and in Doppler doubling of each transition line.

Spectra were observed between 7 and 23 GHz. A Loran frequency standard accurate to 1 part in 10^{10} was used as reference for all line frequency measurements. The observed line widths were $7-10$ kHz (fwhm), and the reported line frequencies have an estimated accuracy of ± 1 kHz.
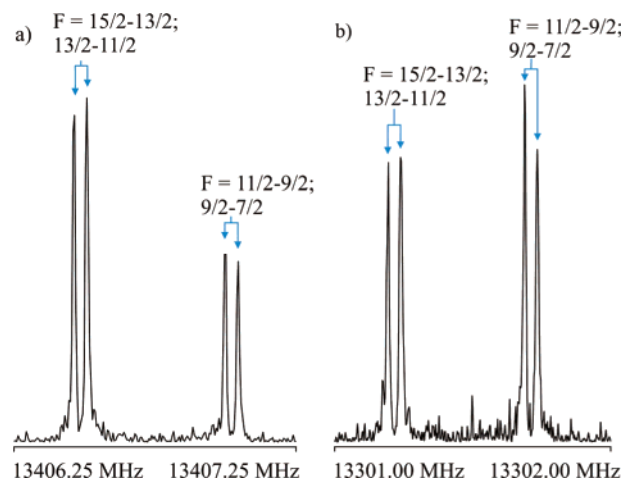
3. Quantum Chemical Calculations

Quantum chemical results reported in ref 11 produced geometries and dissociation energies of noble gas−noble metal halides but lacked valence orbital populations and MOLDEN plots. A new set of MP2[14] calculations has therefore been carried out. The GAUSSIAN 03[15] suite of programs has been used for the XeCuX complexes. For F, the 6-311G** basis set was used.[16] For Xe, pseudopotentials of the Stuttgart/Koeln group were used with corresponding basis sets. The ECP46MWB scheme was employed with the contraction (6s6p3d1f)/4s4p3d1f.[17,18] For Cl, the (631111s/52111p) McLean−Chandler basis set[19] was used, augmented with one d-polarization function ($\alpha_d = 0.75$).[20] The basis set for the Cu atom used an effective core potential (ECP) which left 19 valence electrons ($3s^2 3p^6 3d^{10} 4s^1$). The ECP and the optimized Gaussian basis set (31111s/22111p/411d) were taken from Andrae et al.[21] The Cu basis set was augmented with two f-functions, $\alpha_f = 3.1235$ and $\alpha_f = 1.3375$.[20]

Basis set superposition error (BSSE) was accounted for using the counterpoise correction method of Boys and Bernardi.[22] Local energy densities, $H_b(r)$, have been evaluated at the $(3,-1)$ critical points, located between the Xe and Cu atoms, using Bader's AIMPAC software.[23]

4. Results

4.1. Spectrum and Analysis. A prediction of a rotational constant for XeCuF was made from the ab initio bond lengths reported by Lovallo and Klobukowski.[11] It was found for XeAgX[9] that the experimental bond lengths (r(Xe−M) and r(M−X)) were consistently shorter than the calculated values, and it was expected that the same would occur with XeCuX. The bond lengths used in the prediction for XeCuF were adjusted accordingly. The initial predicted rotational constant for XeCuCl was obtained from our MP2[14] calculations using the 3-21G(d) basis set for Xe[24] and the basis sets for Cu and Cl as described in the previous section. Similar calculations for XeCuF had yielded a geometry whose bond lengths agreed

(14) Møller, C.; Plesset, M. S. *Phys. Rev.* **1934**, *46*, 618.
(15) Frisch, M. J.; et al. *Gaussian 03*, Revision B.5; Gaussian, Inc.: Wallingford, CT, 2004.
(16) Dunning, T. H., Jr. *J. Chem. Phys.* **1989**, *90*(2), 1007.
(17) http://www.theochem.uni-stuttgart.de/pseudopotentials (2003, pseudopotentials of the Stuttgart/Köln group).
(18) Nicklass, A.; Dolg, M.; Stoll, H.; Preuss, H. *J. Chem. Phys.* **1995**, *102*, 8942.
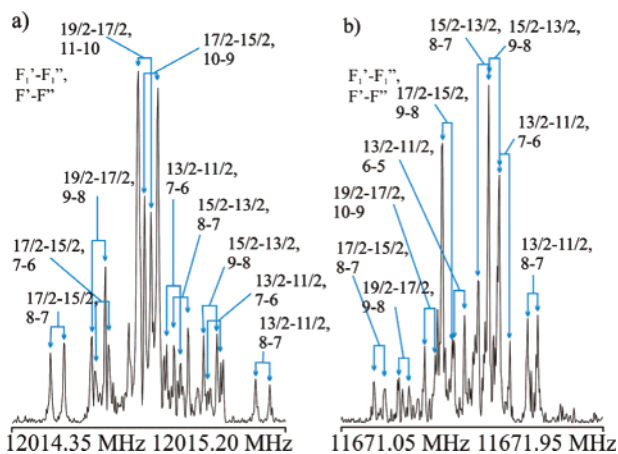(19) McLean, A. D.; Chandler, G. S. *J. Chem. Phys.* **1980**, *72*, 5639.
(20) Antes, I.; Dapprich, S.; Frenking, G.; Schwerdtfeger, P. *Inorg. Chem.* **1996**, *35*, 2089.
(21) Andrae, D.; Häusermann, V.; Dolg, M.; Stoll, M.; Preuss, H. *Theor. Chim. Acta* **1990**, *27*, 213.
(22) Boys, S. F.; Bernardi, F. *Mol. Phys.* **1970**, *19*, 553.
(23) Bader, R. F. W. http://www.chemistry.mcmaster.ca/aimpac (1995).
(24) Dobbs, K. D.; Hehere, W. J. *J. Comput. Chem.* **1986**, *7*, 359.

Figure 1. Portion of the observed hyperfine structure in the $J = 6-5$ transition of $^{132}Xe^{63}CuF$ and $^{132}Xe^{65}CuF$. Respectively, 1000 and 5000 averaging cycles were taken over 4K data points; 8K transform was used. Quantum numbers F′−F″ from coupling scheme $\mathbf{J} + \mathbf{I}_{Cu} = \mathbf{F}$.

within 0.02 Å with experiment, and comparable agreement was expected for XeCuCl. Initial experimental conditions for the preparation of XeCuX were predicted from conditions required to prepare ArCuX[2] and KrCuX.[8]

The first transitions found for XeCuF were within 40 MHz of the initial predicted frequencies and within 100 MHz for XeCuCl. Both complexes have spectra showing the "comb" of equally spaced groups of lines characteristic of linear molecules. The spectra were confirmed to be from the XeCuX complexes on the following basis. First, both spectra required the ablation of the Cu rod and the presence of the precursor gases (SF_6 or Cl_2 and Xe). Second, the transitions of XeCuF were consistent with nuclear quadrupole splitting from Cu ($I = {}^3/_2$). The transitions of XeCuCl showed additional nuclear quadrupole splitting from Cl ($I = {}^3/_2$). Third, the numbers and relative abundances of Xe, Cu, and Cl isotopes were observed in the spectra. Fourth, all transitions assigned to complexes containing ^{131}Xe ($I = {}^3/_2$) showed additional complexity from xenon hyperfine splitting. The line frequencies and quantum number assignments can be found in the Supporting Information. The coupling scheme for molecules with one quadrupolar nucleus is $\mathbf{J} + \mathbf{I} = \mathbf{F}$, where $\mathbf{I}$ is the nuclear spin angular momentum of the nucleus in question. When two quadrupolar nuclei are involved in a molecule, the coupling scheme is $\mathbf{J} + \mathbf{I}_1 = \mathbf{F}_1$; $\mathbf{F}_1 + \mathbf{I}_2 = \mathbf{F}$, where the splitting due to the nucleus 1 ($\mathbf{I}_1$) is greater than that due to nucleus 2 ($\mathbf{I}_2$). The coupling scheme for molecules with three quadrupolar nuclei follows a similar sequence and hierarchy: $\mathbf{J} + \mathbf{I}_1 = \mathbf{F}_1$; $\mathbf{F}_1 + \mathbf{I}_2 = \mathbf{F}_2$; $\mathbf{F}_2 + \mathbf{I}_3 = \mathbf{F}$. Representative transitions for XeCuF are shown in Figure 1 and for XeCuCl in Figure 2. Spectra presented for XeCuF show the difference in hyperfine splitting for the Cu isotopes. The difference in splitting caused by the Cl isotopes can be seen in the XeCuCl spectra. Transitions containing splitting due to ^{131}Xe are shown in Figures 3 and 4 for $^{131}XeCuF$ and $^{131}XeCuCl$, respectively.

No magnetic hyperfine structure from ^{129}Xe or F (both with $I = {}^1/_2$) was observed. The analyses were carried out with rotational (B_o) and centrifugal distortion (D_J) constants, plus, where necessary, nuclear quadrupole coupling (eQq) and nuclear spin-rotation (C_I) constants. The spectra for each isotopomer were analyzed individually using Pickett's global least-squares

Figure 2. Portion of the observed hyperfine structure in the $J = 8-7$ transition of $^{132}Xe^{63}Cu^{35}Cl$ and $^{132}Xe^{63}Cu^{37}Cl$. Respectively, 4100 and 19 000 averaging cycles were taken over 4K data points; 8K transform was used. Quantum numbers $F_1'-F_1''$, $F'-F''$ from coupling scheme $\mathbf{J} + \mathbf{I}_{Cu} = \mathbf{F}_1$, $\mathbf{F}_1 + \mathbf{I}_{Cl} = \mathbf{F}$.
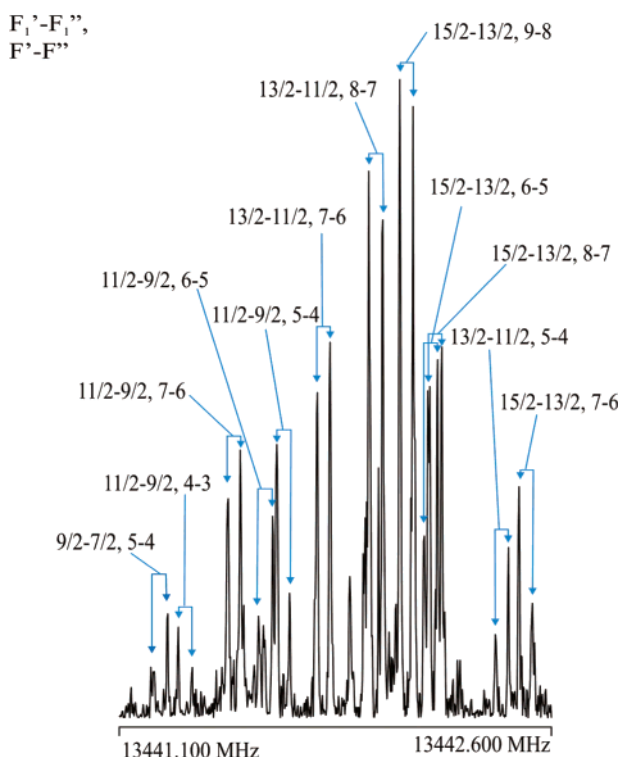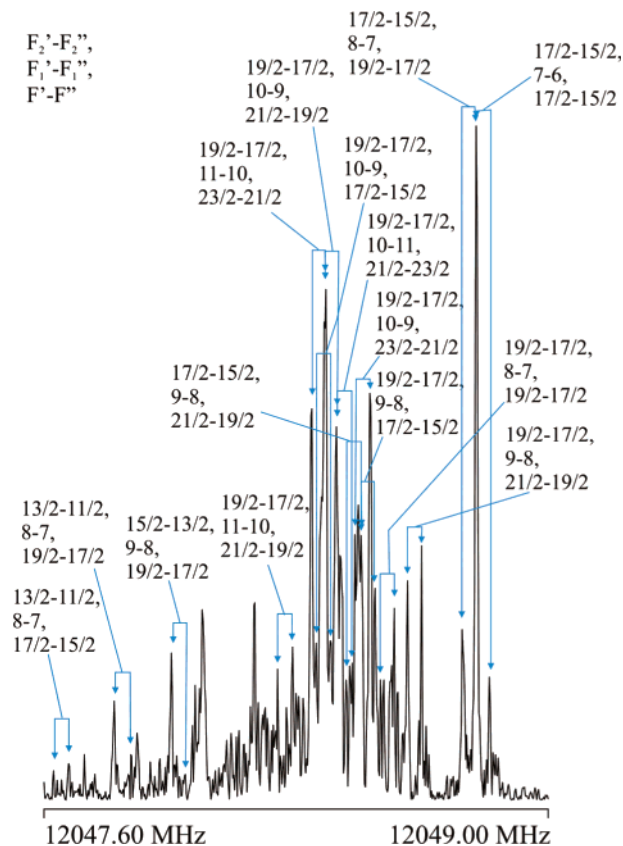

Figure 3. Portion of the observed hyperfine structure in the $J = 6-5$ transition of $^{131}Xe^{63}CuF$. A total of 25 250 averaging cycles was taken over 4K data points; 8K transform was used. Quantum numbers $F_1'-F_1''$, $F'-F''$ from coupling scheme $\mathbf{J} + \mathbf{I}_{Xe} = \mathbf{F}_1$, $\mathbf{F}_1 + \mathbf{I}_{Cu} = \mathbf{F}$.

Figure 4. Portion of the observed hyperfine structure in the $J = 8-7$ transition of $^{131}Xe^{63}Cu^{35}Cl$. A total of 25 150 averaging cycles was taken over 4K data points; 8K transform was used. Quantum numbers $F_2'-F_2''$, $F_1'-F_1''$, $F'-F''$ from coupling scheme $\mathbf{J} + \mathbf{I}_{Xe} = \mathbf{F}_1$, $\mathbf{F}_1 + \mathbf{I}_{Cu} = \mathbf{F}_2$, $\mathbf{F}_2 + \mathbf{I}_{Cl} = \mathbf{F}$.

fitting program, SPFIT.[25] The spectroscopic constants for each isotopomer are given in Table 1 for XeCuF and in Table 2 for XeCuCl.

4.2. Structures of the Molecules. The spectra show both XeCuF and XeCuCl to be linear. The rotational constants from Tables 1 and 2 were used to determine their bond lengths. The equilibrium (r_e) geometries cannot be precisely determined since rotational transitions were observed in the ground vibrational state only and approximations had to be made.

Geometries have been obtained using four different approximations. First, the ground-state effective (r_o) structures have been determined from least-squares fits to the ground-state

moments of inertia (I_o); these fits ignore any vibrational or isotopic dependence. In the second method, the vibrational dependence was partially accounted for using the following equation for the ground-state moments of inertia:[26]

$$I_o = I_{rigid}(r_{I\epsilon}) + \epsilon \tag{1}$$

where I_{rigid} is an approximation to the equilibrium moment of inertia and ϵ is an additional fitting parameter in the least-squares fit. These produced an $r_{I\epsilon}$ geometry; it is believed to provide a better approximation to the equilibrium values than the r_o values. Unfortunately, an isotopic dependence remains with ϵ.

In 1999, Watson et al.[27] developed the mass-dependent (r_m) geometries by accounting for the isotopic dependence of ϵ in the following equation for the ground-state moments of inertia:

$$I_o = I_{rigid}(r_m) + cI_{rigid}^{1/2} + d\left[\frac{m_1 m_2 m_3}{m_1 + m_2 + m_3}\right]^{1/4} \tag{2}$$

where c and d are fitting parameters and m_1, m_2, and m_3 are the masses of the atoms. The $r_m^{(1)}$ structures are obtained by setting $d = 0$ and fitting to the bond lengths and c. When the fit includes d also, the $r_m^{(2)}$ geometries are obtained. The $r_m^{(2)}$ bond lengths

(25) Pickett, H. M. *J. Mol. Spectrosc.* **1991**, *148*, 371.
(26) Rudolph, H. D. *Struct. Chem.* **1991**, *2*, 581.
(27) Watson, J. K. G.; Roytburg, A.; Ulrich, W. *J. Mol. Spectrosc.* **1999**, *196*, 102.

Table 1. Spectroscopic Constants of XeCuF

parameter	^{129}Xe^{63}Cu^{19}F	^{131}Xe^{63}Cu^{19}F	^{132}Xe^{63}Cu^{19}F	^{134}Xe^{63}Cu^{19}F	^{136}Xe^{63}Cu^{19}F	^{129}Xe^{65}Cu^{19}F	^{132}Xe^{65}Cu^{19}F
B_o (MHz)	1126.1926(3)[a]	1120.1761(2)	1117.2361(1)	1111.4750(3)	1105.8760(3)	1117.4820(3)	1108.4624(3)
D_J (kHz)	0.204(5)	0.207(3)	0.1967(8)	0.192(5)	0.193(5)	0.204(5)	0.193(5)
eQq(Cu) (MHz)	47.62(8)	47.77(6)	47.76(11)	47.77(8)	47.66(8)	44.06(8)	44.18(8)
eQq(^{131}Xe) (MHz)		−87.78(7)					
C_I(Cu) (kHz)	4.29[b]	4.29[b]	4.29(95)	4.29[b]	4.29[b]	4.59[c]	4.59[c]

[a] Numbers in parentheses are one standard deviation in units of the last significant figure. [b] Fixed at the value for ^{132}Xe^{63}Cu^{19}F. [c] Fixed at the value for ^{132}Xe^{63}Cu^{19}F, scaled by the ratio of the product of the ^{65}Cu and ^{63}Cu magnetic moments and the rotational constants.

Table 2. Spectroscopic Constants of XeCuCl

parameter	^{129}Xe^{63}Cu^{35}Cl	^{131}Xe^{63}Cu^{35}Cl	^{132}Xe^{63}Cu^{35}Cl	^{134}Xe^{63}Cu^{35}Cl	^{136}Xe^{63}Cu^{35}Cl	^{129}Xe^{65}Cu^{35}Cl	^{132}Xe^{65}Cu^{35}Cl	^{132}Xe^{63}Cu^{37}Cl
B_o (MHz)	757.30669(9)[a]	753.0300(2)	750.93467(5)	746.8318(2)	742.8423(2)	754.6708(2)	748.2566(1)	729.4729(3)
D_J (kHz)	0.0794(7)	0.104(2)	0.0782(4)	0.073(1)	0.076(1)	0.073(2)	0.078(1)	0.070(2)
eQq(Cu) (MHz)	41.81(9)	41.6(1)	41.57(6)	41.6(2)	41.3(2)	38.7(2)	38.1(1)	41.2(2)
eQq(Cl) (MHz)	−26.10(6)	−26.4(1)	−26.01(4)	−25.90(7)	−25.92(7)	−26.04(9)	−26.04(6)	−20.5(1)
eQq(^{131}Xe) (MHz)		−81.4(2)						

[a] Numbers in parentheses are one standard deviation in units of the last significant figure.

Table 3. Geometry[a] of XeCuF

method	r(Xe–Cu)	r(Cu–F)	comments
r_o	2.4327(5)[b]	1.754(1)	
$r_{I\epsilon}$	2.43231(3)	1.7507(1)	$\epsilon = 0.493(12)$ u Å^2
$r_m^{(1)}$	2.43099(5)	1.7498(1)	$c = 0.0463(12)$ u$^{1/2}$ Å
$r_m^{(2)}$	2.42978(5)	1.744923[c]	$c = 0.149(2)$ u$^{1/2}$ Å;
			$d = −0.244(6)$ u$^{1/2}$ Å^2
MP2	2.456	1.732	
MP2[d]	2.459	1.737	

[a] Bond distances in Å. [b] Numbers in parentheses are one standard deviation in units of the last significant figure. [c] In the $r_m^{(2)}$ geometry, the CuF internuclear distance was fixed at the r_e of CuF.[28] [d] Values predicted in ref 11.

Table 4. Geometry[a] of XeCuCl

method	r(Xe–Cu)	r(Cu–Cl)	comments
r_o	2.471(7)[b]	2.058(1)	
$r_{I\epsilon}$	2.4687(5)	2.0589(4)	$\epsilon = 0.80(11)$ u Å^2
$r_m^{(1)}$	2.4672(6)	2.0577(4)	$c = 0.062(8)$ u$^{1/2}$ Å
$r_m^{(2)}$	2.4669(4)	2.0572(3)	$c = 0.104(13)$ u$^{1/2}$ Å;
			$d = −0.144(42)$ u$^{1/2}$ Å^2
MP2	2.4939	2.0482	
MP2[c]	2.497	2.060	
r_e(CuCl)[d]		2.051177(8)	

[a] Bond distances in Å. [b] Numbers in parentheses are one standard deviation in units of the last significant figure. [c] Reference 11. [d] Reference 29.

Table 5. NgM Bond Lengths (r), Centrifugal Distortion Constants (D_J), NgM Stretching Frequencies (ω), and Force Constants (k) of XeCuX and Related Compounds and Complexes[a]

	r(NgM) (Å)		D_J	ω(NgM) (cm^{-1})		k(NgM)
complex	expt	ab initio	(×10^2 kHz)	expt[b]	calcd	(Nm^{-1})[c]
ArCuF[d]	2.22[e]	2.24	94	224	228	79
ArCuCl[d]	2.27[e]	2.30	34	197	190	65
KrCuF[f]	2.32	2.32	38	185	198	84
KrCuCl[f]	2.36	2.37	15	162	148	70
XeCuF[g]	2.43	2.46	20	178	169	94
XeCuCl[g]	2.47	2.50	8	155	146	80
ArAgF[h]	2.56[e]	2.59	95	141	127	36
KrAgF[i]	2.59	2.61	31	125	113	48
XeAgF[j]	2.66	2.68	14	130	108	64
XeAgCl[j]	2.70	2.73	6	120	99	58
ArAuF[k]	2.39[e]	2.40	51	221	214	97
KrAuF[l]	2.46[m]	2.45	16	176	184	110
XeAuF[n]	2.54[m]	2.55	7	164	165	137
Ar−NaCl[o]	2.89		900	21		0.6
ArHg[p]	4.05				22	
Ar−HF[q]	2.92		7210	42		
Kr−HF[r]	2.93		3190	43		
Xe−HF[s]	3.07		1820	45		

[a] All values given are from the reference indicated with the molecular formula, except for the ab initio values of r(NgM), which are from ref 11. [b] Calculated from D_J using a diatomic approximation. [c] Force constant k derived from ω(NgM) using a diatomic approximation. [d] Reference 2. [e] r_o structure. [f] Reference 8. [g] This work. [h] Reference 1 or 7, except where stated otherwise. [i] Reference 5 or 7, except where stated otherwise. [j] Reference 9. [k] Reference 3. [l] Reference 7, unless otherwise stated. [m] $r_m^{(1)}$ structure. [n] Reference 10. [o]Reference 30. [p] Reference 31. [q] Reference 39. [r] Reference 32. [s] Reference 33.

are believed to provide the most reliable approximation to the equilibrium geometry from ground-state data alone.[27]

The results of the fits and of the ab initio calculations for XeCuF and XeCuCl are given in Tables 3 and 4, respectively. The CuF bond length of XeCuF was fixed to the monomeric value in the $r_m^{(2)}$ structure since the unconstrained fit produced highly correlated, poorly determined values, probably because no isotopic substitution could be done on fluorine. The fit with the fixed CuF bond length produced satisfactory results. The bond lengths obtained are in agreement with the ab initio values. The XeCu bond is short in both complexes.

5. Discussion

5.1. Xenon−Copper Bond Length. The most important property of the noble gas−noble metal halides is perhaps the short noble gas-to-metal bond length. This property was first noticed with ArAgCl[1] and continues to be observed in all other

NgMX molecules. Table 5 shows the experimental and ab initio NgM bond lengths for a number of NgMX molecules. The XeCu bond lengths follow the established trends. The XeCu bond length is shorter in XeCuF than in XeCuCl, consistent with the other NgCuX molecules. The XeCu bonds are slightly longer than the corresponding KrCu and ArCu bonds, as expected from studies on NgAgX and NgAuX. The XeCu bonds are also shorter than XeAu and XeAg bonds, again confirming trends from previous experiments and ab initio calculations. For all NgMX molecules, the bond lengths are quite short in comparison to those of the van der Waals complexes Ar−NaCl,[30]

(28) Hoeft, J.; Lovas, F. J.; Tiemann, E.; Törring, T. *Z. Naturforsch.* **1970**, *25a*, 35.
(29) Manson, E. L.; DeLucia, F. C.; Gordy, W. *J. Chem. Phys.* **1975**, *62*, 1040.
(30) Mizoguchi, A.; Endo, Y.; Ohshima, Y. *J. Chem. Phys.* **1998**, *109*, 10539.

Table 6. Comparison of Noble Gas−Noble Metal Bond Lengths (Å) in NgMX Complexes with Values Estimated from Standard Parameters

	Standard Parameters		
atom/ion	van der Waals radius (r_{vdW})[a]	ionic radius (r_{ion})	covalent radius (r_{cov})
Ar	1.88		0.94−0.95[b] (0.98)[c]
Kr	2.00		1.09−1.11[b]
Xe	2.18		1.30−1.31[b]
Cu+/Cu(I)		0.60[d]	1.06[e]
Ag+/Ag(I)		0.81[d]	1.28[e]
Au+/Au(I)		0.77[d]	1.27[e]
Na+		0.79[d]	

	Bond Lengths r(NgM) in NgMX		
	r_{vdW}(Ng) + r_{ion}(M+)	expt	r_{cov}(Ng) + r_{cov}(M(I))
ArCuX	2.48	2.22−2.30[f]	2.04
KrCuX	2.60	2.32−2.36[g] ...[h]	2.16
XeCuX	2.78	2.43−2.47[i] ...	2.37
ArAgX	2.69 ...	2.56−2.64[j]	2.26
KrAgX	2.81	2.59−2.66[k]	2.38
XeAgX	2.99	2.65−2.70[l] ...	2.58
ArAuX	2.65	2.39−2.50[m]	2.25
KrAuX	2.77	2.46−2.52[n] ...	2.37
XeAuF	2.95	2.54[o] ...	2.57
Ar−NaCl	2.67	2.89[p]	

[a] Reference 34. [b] Reference 36. [c] Reference 37. [d] These are the values for coordination number 2. All are calculated from r(M+) = r(MF) − r(F−). The values for Cu+ and Ag+ are from ref 35; those for Au+ and Na+ are from ref 8. [e] Reference 38. [f] Reference 2. [g] Reference 8. [h] Dots show which sum of radii is closer to the experimental bond lengths. [i] This work. [j] Reference 1. [k] References 5−7. [l] Reference 9. [m] References 3 and 4. [n] References 4 and 7. [o] Reference 10. [p] Reference 30.

ArHg,[31] Kr−HF,[32] and Xe−HF.[33] The short bond lengths are reproduced by both sets of ab initio calculations.

Comparing the NgM bond lengths in various NgMX is difficult because of the differences in the sizes of the noble gases and noble metals. Table 6, an expansion of Table 11 from ref 7, shows standard parameters with which to compare experimental bond lengths. The first limit, which can be considered the van der Waals limit, is the sum of the noble gas van der Waals radius[34] and the M+ ionic radius.[7,35] The second limit, considered the covalent limit, is the sum of noble gas and M(I) covalent radii.[36−38] Both of these limits are simply benchmark values and should not be considered as hard and fast rules. The experimental bond lengths are expressed as the range of values obtained for the different halides. For all molecules in the series (except XeAuF),[10] the experimental bond length values are less than the van der Waals limits and greater than the covalent limits. The experimental XeCu bond lengths for XeCuF and XeCuCl are very close to the covalent limit and well below the van der Waals limit.

It should be noted that the experimental bond length for the van der Waals complex Ar−NaCl[30] is larger than the van der

(31) Ohshima, Y.; Iida, M.; Endo, Y. *J. Chem. Phys.* **1990**, *92*, 3990.
(32) Buxton, L. W.; Campbell, E. J.; Keenan, M. R.; Balle, T. J.; Flygare, W. H. *Chem. Phys.* **1981**, *54*, 173.
(33) Baiocchi, F. A.; Dixon, T. A.; Joyner, C. H.; Klemperer, W. *J. Chem. Phys.* **1981**, *75*, 2041.
(34) Pyykkö, P. *Chem. Rev.* **1997**, *97*, 597.
(35) Huheey, J. E.; Keiter, E. A.; Keiter, R. L. *Inorganic Chemistry, Principles of Structure and Reactivity*, 4th ed.; Harper-Collins: New York, 1993.
(36) Pyykkö, P. *Science* **2000**, *290*, 117.
(37) Bartlett, N.; Sladky, F. O. In *Comprehensive Inorganic Chemistry*; Bailar, J. C., Eméleús, H. J., Nyholm, R., Trotman-Dickenson, A. F., Eds.; Pergamon: Oxford, 1973.
(38) Pyykkö, P. *Chem. Rev.* **1988**, *88*, 579.

Waals limit as defined here. The dots (...) in the table indicate when the experimental value is approaching one limit or the other. Table 6 clearly demonstrates the increase in strength of the bonding as the noble gas is changed from Ar to Kr to Xe. All Xe−metal bonds are near the covalent limits. The trend of the strengths of the interactions as the metal is changed can also be seen in the table; they increase as the metal is changed from Ag to Cu to Au.

5.2. Flexibility and Bond Energy of XeCuX. The small centrifugal distortion constants obtained for both XeCuF and XeCuCl indicate that the molecules are highly rigid. These constants are smaller by at least an order of magnitude than the values obtained for typical van der Waals complexes. The values for the centrifugal distortion constants, stretching frequencies, and force constants obtained for several NgMX molecules and various related species are given in Table 5.

The stretching frequencies ω(NgM) are obtained from the diatomic approximation:

$$\omega = \left(\frac{4B^3}{D_J}\right)^{1/2} \quad (3)$$

The results for ω(XeCu) follow the overall pattern established from previous studies. There is good agreement between the experimental and ab initio stretching frequencies.

Both centrifugal distortion constants and stretching frequencies have a mass dependence that complicates comparisons. Evaluating the stretching force constants k(NgM) using

$$k = \frac{16\pi^2 \mu B^3}{D_J} \quad (4)$$

removes the mass dependence and provides a clearer picture of the rigidity of the molecules. The values obtained for the XeCuF and XeCuCl molecules fit the established trends. The XeCu bond in XeCuF is more rigid than in XeCuCl. The XeCu bond is also more rigid than the KrCu and ArCu bonds. The rigidity of the Au-containing molecules is the greatest, followed by the Cu-containing molecules and then by the Ag-containing molecules. The force constants in the NgMX molecules are 2 orders of magnitude greater than k(Ar−Na) in Ar−NaCl.[30]

Table 7 contains NgM dissociation energies D_e for NgMX molecules and related species, obtained in both sets of ab initio studies. The two studies agree fairly well in general. The dissociation energies obtained for XeCuX follow the trends expected. The bond energies are greater for Xe-containing molecules than for the corresponding Kr-containing and Ar-containing molecules. The dissociation energies increase as the metal is changed from Ag to Cu to Au, with Au-containing molecules showing some very large values. The values calculated for the NgMX molecules are much larger than the dissociation energy calculated for the van der Waals complex Ar−NaCl.

Dissociation energies for XeCu+ and XeAg+ ions were calculated in ref 40. Their values (D_e(XeCu+) = 61 kJ mol−1; D_e(XeAg+) = 37 kJ mol−1) agree well with the values obtained for XeMF both in our calculations and from ref 11.

(39) Harris, S. J.; Novick, S. E.; Klemperer, W. *J. Chem. Phys.* **1974**, *60*, 3208.
(40) Freitag, A.; van Wüllen, Ch.; Staemmler, V. *Chem. Phys.* **1995**, *192*, 267.

Table 7. Comparison of MX Dipole Moments and Effective Atomic Charges, Induction Energies and ab Initio Ng−M Dissociation Energies of NgMX Complexes and Related Species

	MX		$-E_{ind}$		D_e	
complex	μ^a	q_{eff}^b	dip.-ind. dip.^{c}	chg.-ind. dip.^{d}	our work	ref 11
ArCuF	5.77^f	0.69	8	22	44^g	37
ArCuCl	5.2^g	0.53	4	13	33^g	28
KrCuF	5.77^f	0.69	9	28	45^h	48
KrCuCl	5.2^g	0.53	5	16	37^h	39
XeCuF	5.77^f	0.69	12	38	63^i	59
XeCuCl	5.2^g	0.53	7	21	55^i	51
ArAgF	6.22^f	0.65	4	11	14^g	18
KrAgF	6.22^f	0.65	5	16	17^g	28
XeAgF	6.22^f	0.65	8	24	36^j	43
ArAuF	3.4^g	0.37	2	5	55^g	50
KrAuF	3.4^g	0.37	3	6	58^g	71
XeAuF	3.4^g	0.37	4	11	101	97
Ar−NaCl	9.00^k	0.79	4	10	8^l	
Ar−BeO	7.2^m	0.84	26	84	45^m	

^{a} μ is the dipole moment (Debye) of the MX monomer. ^{b} q_{eff} is the effective charge of the metal ion to produce the value of μ at the molecular bond length. It is in fractions of an elementary charge. Values from ref 7. ^{c} Dipole-induced dipole induction energy (kJ mol^{-1}). ^{d} Charge-induced dipole induction energy (kJ mol^{-1}). ^{e} D_e in kJ mol^{-1}; BSSE is accounted for, unless otherwise noted. ^{f} Reference 28. ^{g} Reference 7. ^{h} Reference 8. ^{i} This work. ^{j} Reference 9. ^{k} References 41 and 42. ^{l} Reference 30; BSSE is not accounted for. ^{m} Reference 43.
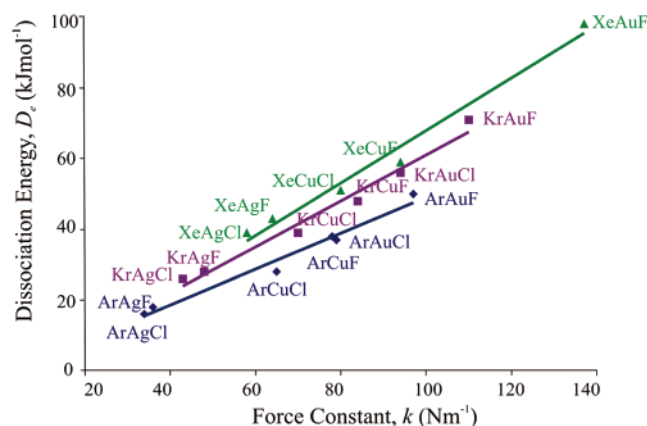
Figure 5. Plot of ab initio dissociation energies, D_e, from ref 11 versus experimental force constants, k(NgM), for the NgMX complexes.

For all the NgMX complexes, there is a monotonic relationship between the NgM dissociation energies and the stretching force constants. Such a relationship is to be expected if the Ng−M bond can be described by a Morse potential where

$$k = 2D_e\beta^2 \qquad (5)$$

and if β, the Morse potential constant, is constant. Figure 5, an expansion of Figure 3 in ref 10, shows a plot of the experimental force constants versus the dissociation energies calculated in ref 11. An approximately linear relationship exists for the NgMX molecules. The measurement of rotational constants and centrifugal distortion constants provides an indirect, approximate measurement of D_e.

To help understand the large calculated Ng−M dissociation energies, purely electrostatic induction energies were also calculated. Two semiempirical methods were used; they are described in detail in ref 7. One was a dipole-induced dipole calculation. The other was a M$^+$−Ng charge-induced dipole calculation, in which the M$^+$ charge was approximated as the effective charge to produce the value of the dipole moment at

Table 8. ^{63}Cu Nuclear Quadrupole Coupling Constants (MHz) in NgCuX Complexes and Related Species

	$eQq(^{63}Cu)$		
molecule	X = F	X = Cl	X = Br
CuX	21.956^a	16.16908^b	12.8510^b
ArCuX	38.056^a	33.186^a	29.92^a
KrCuX	41.77^c	36.52^c	
XeCuX	47.78^d	41.59^d	
XCuX$^-$		61.4^e	57.7^f
OCCuX	75.41^g	70.83^g	67.53^g

^{a} Reference 2. ^{b} Reference 50. ^{c} Reference 8. ^{d} This work. ^{e} Reference 46. ^{f} Reference 47. ^{g} Reference 48.

the MX bond length. Its values can be expected to be reduced by approximately 10% by an X$^-$−Ng term. The resulting induction energies for both calculations are given in Table 7; since the charge-induced dipole terms are much bigger than the dipole-induced dipole terms, the former provide a "worst-case scenario", and discussion is based on them.

The induction energies for XeCuF and XeCuCl again fit the trends found for the other NgMX complexes. For all NgCuX and NgAgX the values are ∼0.5D_e, while those for NgAuX are nearer 0.1D_e. It should be noted that, for the accepted van der Waals complexes Ar−NaCl and Ar−BeO, the induction energies more than account for the calculated D_e values.

Several notes should be made regarding these calculations, as noted in ref 7. They are approximated by a point charge model. They also assume a long-distance approximation which may not be fully valid even for the charge-induced dipole term, and the calculated induction energies could be low as a result by about 50%. In this case, the induction energies would barely exceed the D_e of NgAgX molecules but would not reach those of NgCuX and would be much less than those of NgAuX. There are also several other, smaller, attractive contributions to the induction energy, plus dispersion terms which are comparable to the charge-induced dipole term; however, they are counterbalanced by significant repulsion terms.[44] On the whole, the D_e values cannot be clearly fully accounted for with purely electrostatic interactions, especially for NgAuX and probably also for NgCuX and NgAgX.

5.3. Nuclear Quadrupole Coupling Constants. Nuclear quadrupole coupling constants (NQCCs) have been obtained for copper (^{63}Cu and ^{65}Cu), chlorine (^{35}Cl and ^{37}Cl), and ^{131}Xe. Each provides a probe of the electron distribution at the nucleus in question and how this distribution changes on complex formation.

The NQCCs for ^{63}Cu and ^{65}Cu are in the ratios of their nuclear quadrupole moments (e.g., for ^{132}Xe^{63}CuF and ^{132}Xe^{65}CuF this ratio is 1.081(2), very similar to $eQ(^{63}Cu)/eQ(^{65}Cu) = 1.0806(3)^{45}$). The same situation arises with the NQCCs for ^{35}Cl and ^{37}Cl. Accordingly, the discussion will consider only the ^{63}Cu and ^{35}Cl values.

Table 8 shows the significant changes in $eQq(^{63}Cu)$ values when the noble gas is added to the monomer and as it is changed from Ar to Kr to Xe. The changes to the NQCCs are considered

(41) Hebert, A. J.; Lovas, F. J.; Melendres, C. J.; Hollowell, C. D.; Story, T. L.; Street, K. *J. Chem. Phys.* **1968**, *48*, 2824.
(42) Deleeuw, F. H.; Van Wachem, R.; Dymanus, A. *J. Chem. Phys.* **1969**, *50*, 1393.
(43) Veldkamp, A.; Frenking, G. *Chem. Phys. Lett.* **1994**, *226*, 11.
(44) Bellert, D.; Breckenridge, W. H. *Chem. Rev.* **2002**, *102*, 1595.
(45) Gordy, W.; Cook, R. L. *Microwave Molecular Spectra*, 3rd ed.; Techniques of Chemistry XVIII; Wiley: New York, 1984.

Table 9. [35]Chlorine Quadrupole Coupling Constants (MHz) in CuCl, NgCuCl, and Related Species

molecule	eQq([35]Cl)
CuCl	−32.1229[a]
ArCuCl	−28.032[b]
KrCuCl	−27.30[c]
XeCuCl	−26.01[d]
ClCuCl⁻	−19.3[e]
OCCuCl	−21.474[f]

[a] Reference 49. [b] Reference 2. [c] Reference 8. [d] This work. [e] Reference 47. [f] Reference 48.

Table 10. [131]Xe Nuclear Quadrupole Coupling Constants (MHz) for Various Xe-Containing Species

molecule	eQq([131]Xe)	ref
Xe	0	
Xe−Ne	0.39	53
Xe−Ar	0.72	53
Xe−HCl	−4.9	54
XeCuF	−87.8	this work
XeAgF	−82.8	9
XeAuF	−134.5	10
XeH⁺	−369.5	51
Xe ([Kr]$5s^2 4d^{10} 5p^5 6s^1$)	−505	55

additive rather than multiplicative. For example, addition of Ar to CuX increases eQq([63]Cu) by ∼16 MHz, addition of Kr increases it by ∼20 MHz, while addition of Xe increases it by ∼25 MHz. These changes are ∼38%, ∼45%, and ∼56% of the change when X⁻ is added to form XCuX⁻ ions.[46,47] Similarly, addition of Ar, Kr, and Xe causes changes of ∼30%, ∼37%, and ∼47% of those values obtained when CO is added to form OCCuX compounds.[48] There are clearly very large redistributions of the electron density of Cu when the noble gases are added to form NgCuX.

The [35]Cl NQCCs are presented in Table 9, along with the values obtained for related species. While it appears that their absolute changes on complex formation are less dramatic than the changes for the eQq([63]Cu) values, their fractional changes are comparable. For example, the change on forming XeCuCl from CuCl[49] is approximately ∼48% of the change on forming ClCuCl⁻ ions.[46] This is comparable to, if a little smaller than, the fractional change in the [63]Cu NQCC (∼56%). The same pattern occurs when comparing the change on forming XeCuCl from CuCl[49] to the change on forming OCCuCl[48] (∼57% for eQq([35]Cl) and ∼47% for eQq([63]Cu)).

The NQCCs for the noble gas provide important information about the electron distribution at the noble gas on molecule formation. The noble gas provides a clear picture of charge rearrangement, since the unbound Xe atom is spherically symmetric, making eQq([131]Xe) = 0. Any nonzero values are indicative of the distortion of the noble gas electron cloud upon molecule formation. A comparison of such values is given in Table 10.

The values of eQq([131]Xe) in XeCuF and XeCuCl are entirely in keeping with those of XeAgX[9] and XeAuF.[10] Since eQq([131]Xe) in XeCuCl follows the same trends as that in XeCuF,

Table 11. [131]Xe Nuclear Quadrupole Coupling Constants Resulting from Polarization Due to External Charges

	q_{eff}[a]	E_{zz} (M)	E_{zz} (X)	E_{zz}[b]	eQq (MHz) calc[c]	eQq (MHz) expt
XeCuF[d]	0.69	−1.385	0.273	−1.112	−51	−87.8
XeCuCl[d]	0.53	−1.017	0.165	−0.852	−39	−81.4
XeAgF[e]	0.65	−0.992	0.187	−0.805	−35	−82.8
XeAgCl[e]	0.56	−0.812	0.130	−0.681	−30	−78.2
XeAuF[f]	0.37	−0.646	0.120	−0.526	−23	−134.5

[a] Fractional charge of the M⁺ and X⁻ ions from Table 7. [b] E_{zz} is the sum of the field gradients at the Xe nucleus due to the M⁺ and X⁻ ions alone (E_{zz}(M) and E_{zz}(X), respectively). Units are 10^{20} V m⁻². [c] Calculated using eqs 6 and 7, with $\gamma^{Xe} = 158$; the second term of eq 6 is negligible. The uncertainty for the Xe coupling constants is ±∼4 MHz. [d] This work. [e] Reference 9. [f] Reference 10.

the discussion will focus on the eQq([131]Xe) value obtained for XeCuF. The nearly nonpolar van der Waals complexes containing noble gas−noble gas bonds[52,53] have very small [131]Xe NQCCs. This indicates that little rearrangement of the electron distribution occurs at the Xe center. The hydrogen-bonded complexes[54] have slightly larger eQq([131]Xe), but those values are not nearly as large as those obtained in the [131]XeMX molecules. The large values obtained in [131]XeMX indicate a much stronger interaction between the noble gas and the metal center. However, the NQCCs for [131]Xe are still quite far from the value of Xe ([Kr]$5s^2 4d^{10} 5p^5 6s^1$).[55] From Table 10, it can be clearly seen that the strength of interaction increases as the metal is changed from Ag to Cu to Au.

As was done with dissociation energies, it is possible to compare the experimental [131]Xe NQCCs with calculated NQCCs resulting simply from polarization of the spherical electron distribution of Xe by the external charges on CuX. The procedure used to do this is also described in ref 7. Essentially, one evaluates the field E_z and the field gradient E_{zz} at the Xe nucleus due to CuX alone and then adjusts for the polarized Xe electrons. This is Sternheimer antishielding,[56,57] and the equations are

$$V_{zz} = (\gamma^{Xe} + 1)E_{zz} + \epsilon^{Xe}E_z{}^2 \qquad (6)$$

and

$$eQq = -eQV_{zz} \qquad (7)$$

where γ^{Xe} and ϵ^{Xe} are Sternheimer shielding parameters (138 ≤ γ^{Xe} ≤ 177 V⁻¹ [refs 54 and 58] and −5 ≤ ϵ^{Xe} ≤ −15 V⁻¹ [refs 9 and 10]). The $\epsilon^{Xe}E_z{}^2$ term is an order of magnitude smaller than the other term in eq 6 and thus is neglected for semiquantitative discussions. The values obtained from this calculation and experimentally for XeCuF and XeCuCl are presented in Table 11 and compared with values obtained for

(46) Bowmaker, G. A.; Brockliss, L. D.; Whiting, R. *Aust. J. Chem.* **1973**, *26*, 29.
(47) Bowmaker, G. A.; Boyd, P. D. W.; Sorrensen, R. J. *J. Chem. Soc., Faraday Trans. 2* **1985**, *81*, 1627.
(48) Walker, N. R.; Gerry, M. C. L. *Inorg. Chem.* **2001**, *40*, 6158.
(49) Hensel, K. D.; Styger, C.; Jäger, W.; Merer, A. J.; Gerry, M. C. L. *J. Chem. Phys.* **1993**, *99*, 3320.
(50) Low, R. J.; Varberg, T. D.; Connelly, J. P.; Auty, A. R.; Howard, B. J.; Brown, J. M. *J. Mol. Spectrosc.* **1993**, *161*, 499.
(51) Peterson, K. A.; Petrmichl, R. H.; McClain, R. L.; Woods, R. C. *J. Chem. Phys.* **1991**, *95*, 2352.
(52) Xu, Y.; Jäger, W.; Djauhari, J.; Gerry, M. C. L. *J. Chem. Phys.* **1995**, *103*, 2827.
(53) Xu, Y.; Jäger, W.; Gerry, M. C. L. *J. Chem. Phys.* **1993**, *99*, 919.
(54) Keenan, M. R.; Buxton, L. W.; Campbell, E. J.; Balle, T. J.; Flygare, W. H. *J. Chem. Phys.* **1980**, *73*, 3523.
(55) Faust, W. L.; McDermott, M. N. *Phys. Rev.* **1961**, *123*, 198.
(56) Foley, H. M.; Sternheimer, R. M.; Tycko, D. *Phys. Rev.* **1954**, *93*, 734 and references therein.
(57) (a) Fowler, P. W.; Lazzeretti, P.; Steiner, E.; Zanasi, R. *Chem. Phys.* **1989**, *133*, 121. (b) Fowler, P. W. *Chem. Phys. Lett.* **1989**, *156*, 494.
(58) Feiock, F. D.; Johnson, W. R. *Phys. Rev.* **1969**, *187*, 39.

Table 12. Changes in Mulliken (M) and Natural Bond Orbital (NBO)[a] Populations on Complex Formation for XeCuF and Related NgMX Complexes

	Ng				M					
	Δn_s		$\Delta n_{p\sigma}$		Δn_s		$\Delta n_{p\sigma}$		$\Delta n_{d\sigma}$	
	M	NBO	M	NBO	M	NBO	M	NBO	M	NBO
ArCuF[b]	0.00	−0.01	−0.08	−0.04	0.12	0.13	0.02	0.00	−0.05	−0.05
KrCuF[c]	−0.01	−0.01	−0.12	−0.05	0.12	0.14	0.04	0.00	−0.04	−0.04
XeCuF[d]	−0.05	−0.02	−0.17	−0.07	0.19	0.14	0.04	0.00	−0.02	−0.03
ArAgF[e]	0.00		−0.04		0.07		0.00		−0.02	
KrAgF[f]	0.00		−0.07		0.09		0.01		−0.03	
XeAgF[g]	0.00	−0.01	−0.04	−0.05	0.07	0.12	0.00	0.00	−0.04	−0.03
ArAuF[h]	0.00		−0.12		0.18		0.05		−0.09	
KrAuF[i]	−0.02		−0.19		0.22		0.07		−0.09	
XeAuF[j]	−0.06	−0.03	−0.24	−0.14	0.14	0.21	0.19	0.00	−0.10	−0.05

[a] NBO populations obtained in this work, except for XeAgF and XeAuF reported in refs 9 and 10, respectively. *[b]* Reference 2. *[c]* Reference 8. *[d]* This work. *[e]* Reference 1. *[f]* Reference 5. *[g]* Reference 9. *[h]* Reference 3. *[i]* Reference 6. *[j]* Reference 10.

other ^{131}XeMX. The entire picture represented by eq 7 accounts for less than 60% of the measured eQq values, suggesting that electrostatics cannot be the sole explanation for the large noble gas eQq values.

An estimate of the degree of donation of electron charge to Cu from Xe can be obtained using the simple theory of Townes and Dailey.[59] The eQq value, given by

$$eQq = eQq_{510}\left(n_\sigma - \frac{n_\pi}{2}\right) \qquad (8)$$

where n_σ and n_π are the populations of the Xe $5p_\sigma$ and $5p_\pi$ orbitals, and eQq_{510} is the coupling constant of a singly occupied 5p orbital ($= 505$ MHz from Table 10). If all Xe → Cu donation is σ-donation, then $n_\pi = 4$, and with $eQq = \sim-85$ MHz, then $n_\sigma = 1.83$. This implies a donation of 0.17 electron from Xe to Cu.

5.4. Ab Initio Calculations. Ab initio calculations produced the bond lengths, vibration frequencies, and NgM dissociation energies discussed earlier (Table 7), along with information regarding the electron distributions of the molecules. Specifically, Mulliken and natural bond orbital (NBO) populations, MOLDEN plots of electron density of valence molecular orbitals, and local energy densities at the bond critical points were obtained. The results from ref 11 agree well with our calculations where they overlap.

The Mulliken and NBO populations have been calculated to show their changes on complex formation. The results for XeCuF and XeCuCl are quite similar, with the changes in values obtained for the fluoride being slightly larger than those for the chloride. Since both follow the same trends, the XeCuF results alone are presented in Table 12. Both the Mulliken and NBO populations follow the same trend, even though the values differ. There is significant donation of $\sim$0.1−0.2 σ-electron density from Xe to Cu. This is consistent with the trends from previous studies of NgMX molecules. It is also consistent with the value of 0.17 electron obtained form $eQq(^{131}$Xe) using the Townes−Dailey model.

Electron density contour plots were generated from the results of the GAUSSIAN 03[15] calculations using the MOLDEN 3.4 program.[60] In particular, plots were generated for the valence molecular orbitals for XeCuF and XeCuCl. The plots for both
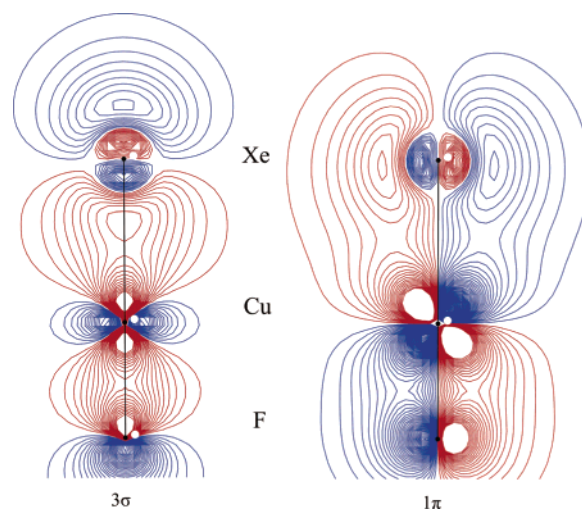
Figure 6. MOLDEN contour diagrams of two occupied valence molecular orbitals of XeCuF; in each case, the value of the contours is $0.02n$, with $n = 1-13$. The different colors indicate opposite signs of the wave functions.

complexes are quite similar, and Figure 6 shows those obtained for XeCuF. The values for the contours are $0.02n$, with $n = 1-13$; the different colors indicate opposite signs for the MO wave functions. Large orbital overlap between Xe and Cu is found for both molecules, consistent with the possibility of XeCu covalent bonding. In both cases, the σ-overlap between Xe ($5p_z$) and Cu ($3d_{z^2}$) is significantly greater than the π-overlap between Xe ($5p_x$) and Cu ($3d_{xz}$), suggesting that any covalent bonding arises primarily from the σ-overlap. It should be mentioned that plots with comparable overlap could not be constructed for the van der Waals complexes Ar−BeO and Ar−NaCl.

A criterion for assessing the character of a bond to a noble gas was suggested by Cremer and Kraka[61] and reviewed in 1990 by Frenking and Cremer.[62] It involves evaluating the so-called local energy density distribution ($H(r)$) at the $(3,-1)$ bond critical point along the path of maximum energy density (MED) between the atoms. $H(r)$ is written as[61,63]

$$H(r) = G(r) + V(r) \qquad (9)$$

where $G(r)$ is the local kinetic energy distribution and $V(r)$ is the local potential energy distribution. If $H(r)$ is negative at the

(59) Townes, C. H.; Dailey, B. P. *J. Chem. Phys.* **1949**, *17*, 782.
(60) Schaftenaar, G. MOLDEN 3.4, CAOS/CAMM Center, The Netherlands, 1998.

(61) Cremer, D.; Kraka, E. *Angew. Chem.* **1984**, *96*, 612. See also: Cremer, D.; Kraka, E. *Angew. Chem., Int. Ed. Engl.* **1984**, *23*, 627.
(62) Frenking, G.; Cremer, D. *Struct. Bonding* **1990**, *73*, 18−95.
(63) Cremer, D.; Kraka, E. *Croat. Chem. Acta* **1984**, *57*, 1259.

bond critical point, then the potential energy dominates and electron density will accumulate to give a covalent bond. On the other hand, if $H(r)$ is zero or positive, the interaction will be closed-shell, as in ionic bonding, van der Waals bonding, or hydrogen bonding.[63] The bond critical point can be considered as the point at which there are equal contributions overall to the molecular orbitals from the atoms involved in the bond. These values were obtained from the wave functions from results of ab initio calculations using Bader's program AIMPAC, obtained from ref 23. For XeCuX, the MED path is a straight line between the nuclei; at the XeCu bond critical point, $H(r)$ = −0.070 hartree Å^{-3} for XeCuF and $H(r)$ = −0.067 hartree Å^{-3} for XeCuCl. These results are consistent with the presence of a weak XeCu covalent bond. Similar results have been obtained for XeAuF.[10]

The negative $H(r)$ values are not surprising. Frenking and Cremer pointed out that (ref 62, pp 46−50) a negative $H(r)$ will be found when an ab initio dissociation energy is significantly greater than the corresponding charge-induced dipole induction energy. This is clearly the case for the NgMX complexes, and particularly for XeCuF and XeCuCl.

6. Conclusion

XeCuF and XeCuCl have been detected and characterized using gas-phase microwave rotational spectroscopy. In the series NgMX, with Ng = Ar, Kr, Xe and M = Cu, Ag, Au, they provide the last remaining NgM bond to be found. Complexes with all other NgM combinations had been reported earlier. The XeCu bonds have been found to be very strong, second in strength only to the XeAu bond in XeAuF.

The XeCu bonds are short, only slightly longer (0.06−0.1 Å) than a benchmark XeCu covalent bond, and much shorter (by more than 0.3 Å) than a benchmark van der Waals bond.

They are also rigid, with large stretching frequencies and force constants. The nuclear quadrupole coupling constants for Cu, Cl, and ^{131}Xe are all consistent with a major redistribution of electron density on complex formation. The changes in the Cu and Cl coupling constants are about 50% of those found when Cl$^-$ adds to CuCl to form ClCuCl$^-$. The ^{131}Xe coupling constants cannot be accounted for in terms of a simple electrostatic interaction. By the Townes−Dailey model they are consistent with donations of ∼0.17 electron from Xe to Cu.

Ab initio XeCu dissociation energies ∼55−60 kJ mol^{-1} cannot be accounted for by simple electrostatics. Both Mulliken and natural bond orbital populations suggest electron donation from Xe to Cu, consistent with the Townes−Dailey results. MOLDEN plots of occupied valence molecular orbitals show significant electron sharing between Xe and Cu. Negative local energy densities at the XeCu bond critical points have been calculated for both XeCuF and XeCuCl.

All the evidence, both experimental and theoretical, is consistent with XeCu covalent bonding. Although the XeCu bonds are among the strongest NgM bonds, and the strongest not involving Au, they are nonetheless rare. To our knowledge, no other species with such bonds have been detected and certainly no other neutral molecules. It will be interesting if other molecules with XeCu covalent bonds can be formed.

Supporting Information Available: Complete citation of ref 15 and measured transition frequencies. This material is available free of charge via the Internet at http://pubs.acs.org.

JA060745Q